ELSEVIER

Journal of Nuclear Materials 251 (1997) 139–144

journal of nuclear materials

STM and AFM investigations of surface structures following swift heavy ion irradiation

K. Havancsák [a,*], L.P Biró [b], J. Gyulai [b], Z. Illés [a]

[a] *Institute for Solid State Physics, Eötvös University, Múzeum krt. 6-8, H-1088 Budapest, Hungary*
[b] *KFKI Research Institute for Materials Science, P.O. Box 49, H-1525 Budapest, Hungary*

Abstract

Samples of highly oriented pyrolitic graphite, muscovite mica and (100) oriented silicon were irradiated with 209 MeV Kr ions. The irradiations were performed in a perpendicular direction to the sample surface. The irradiation fluence used was 10^{12} ions/cm^2. Scanning tunnelling microscope (STM) and atomic force microscope (AFM) observations were accomplished without any further sample preparation. Experimental observations are compared to computer simulations (TRIM code) and primary knock-on atomic spectrum calculations (LET code). Surface features observed on different materials are characterised and compared to each other. Distinction can be made between surface features attributed to nuclear stopping effects and defects owing to electronic stopping mechanisms. © 1997 Elsevier Science B.V.

1. Introduction

In the last decade good progress has been made towards a better understanding of the nature of damage produced by swift heavy ions in solids. Damage production in metals is mostly a well-understood process. The main damage creating process in metals is elastic collision, although the irradiations of metals with heavy ions of GeV energy are exceptions to this rule [1], since high local electronic excitations can produce structural modifications as well. In semiconductors and insulators the inelastic interactions between the impinging charged particle and the electrons in the solid target play the significant role. The existing theoretical models for electronic stopping, i.e. the Coulomb explosion model [2] and the thermal spike model [3], have partial successes in describing experimental results, but a lot of details have not been clarified yet [4].

In the case of insulators the most frequently used experimental techniques in irradiation damage investigation are chemical etching and transmission electron microscopy. The drawback of etching is the loss of information in the damaged region, owing to the chemical interaction [5].

Recently scanning probe methods, such as scanning tunneling microscopy (STM) and atomic force microscopy (AFM) have offered a way to the direct observation of irradiation defects at atomic scale. These are invaluable methods for investigation of the irradiation surface structures at nanometer scale. Nevertheless, they are surface bond techniques which is their main drawback. To some extent, these two methods are complementary to each other. STM is sensitive not only to surface topography, but to the spatial variation of electronic density near the Fermi surface. Samples must be conductive for STM imaging. On the other hand, an AFM image represents a picture of the total charge density, whereby in contact measuring mode the measured corrugation, as a first approximation, gives information about the atomic order. AFM images in tapping mode, besides surface topography, represent the local modifications of elastic properties, too. For AFM imaging no conducting sample is required. Atomic resolution can be achieved in principle by both methods, nevertheless, STM offers an easier way.

Irradiation damage structure on graphite surfaces has been investigated by several authors after low energy and swift heavy ion irradiation using STM and AFM [6–11]. The interest in the investigation of this material is motivated, on the one hand, by its use in nuclear reactors and on the other hand by the fact that graphite is a suitable substance for surface investigation. Graphite is a layered

* Corresponding author. E-mail: havancsak@ludens.elte.hu.

PII S0022-3115(97)00259-6

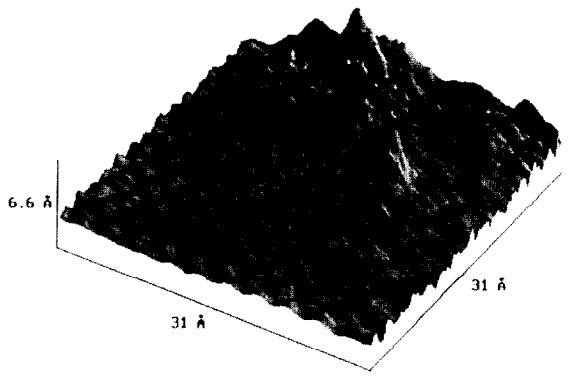

Fig. 1. Atomic resolution 3D STM image of graphite showing hills of the smallest size. Window of 3.1×3.1 nm, vertical scale of 0.66 nm. The regular corrugation in the lower part of the image corresponds to the graphite atomic order.

material which means that strongly bonded atoms are arranged in planes exhibiting weak interplanar bonding strength. That is why it cleaves easily exposing clean, atomically flat terraces for scanning probe measurements.

In a previous paper [9] the nature of all visible surface features on highly oriented pyrolitic graphite (HOPG) has been studied after 215 MeV Ne ion irradiation, using STM imaging. The main surface defects found were hills (called in Ref. [9] as type I structure), which have been associated with the nuclear collision cascades, originating from the primary knock-on carbon atoms beneath the surface. The typical geometrical extensions of this type of defects were 100–300 nm in diameter and 3–7 nm in height. There was no clear evidence of imaging the electronic cascades of the projectile ion [9], although in some very rare cases crater type surface features were found, which might be attributed to the Ne ions impinging on the graphite surface [11].

Much attention has been paid to track formation by swift heavy ions in muscovite mica (MM) [8,12,13], as this

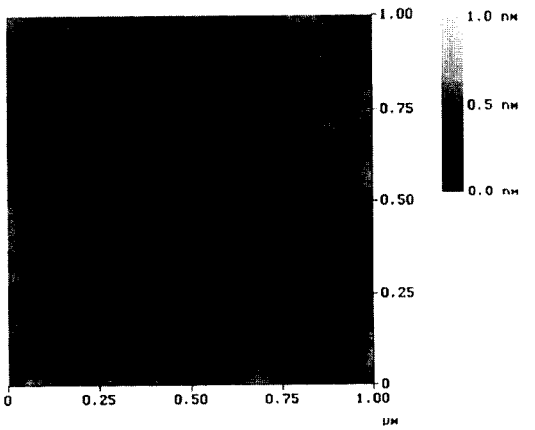

Fig. 2. AFM image of Kr ion irradiated graphite showing hills and holes. Window of 1000×1000 nm^2, grayscale of 1 nm.

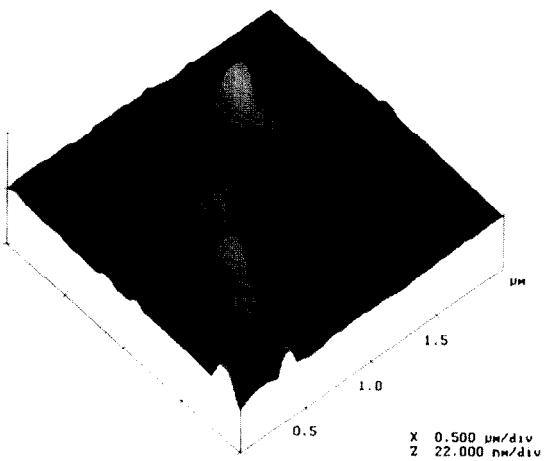

Fig. 3. AFM image of 2000×2000 nm^2, showing surface hills on Kr ion irradiated mica. Vertical scale of 22 nm.

was the first known track recording material. MM is a layered material as well and while HOPG is a relatively good conductor in the c plane, MM is an insulator. MM proves to be a suitable material for atomic force microscopy and for comparison to results obtained in graphite.

In the present work the most frequent surface features on HOPG and MM are treated by extensive STM and AFM investigations after 209 MeV Kr ion irradiation. The third material used in this work is Si, which is a semiconductor. In a most recent work [14], damage production in Si after swift Kr ion irradiation was discussed in detail. In the present paper the most frequent surface features observed on HOPG, MM and Si are compared.

2. Experiment

Freshly cleaved bulk HOPG and MM samples were irradiated in a direction normal to the cleavage plane. The

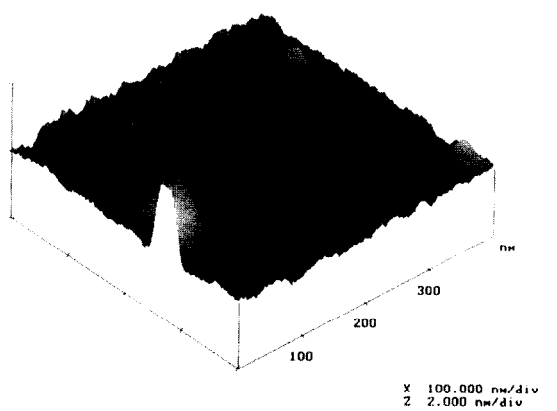

Fig. 4. AFM image of 400×400 nm^2, showing hills on Kr ion irradiated silicon surface. Vertical scale of 2 nm.

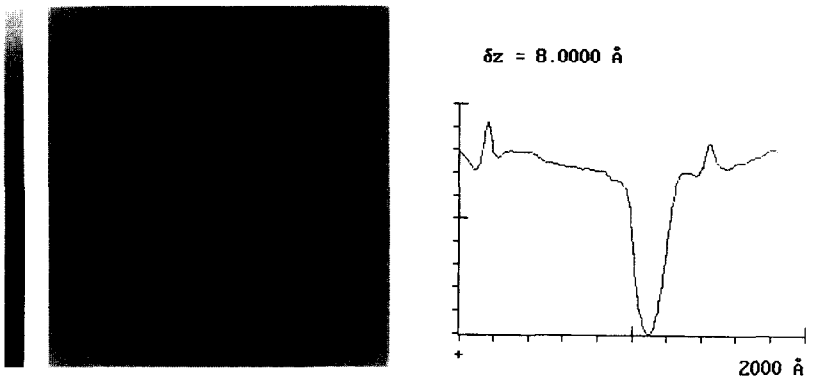

Fig. 5. STM image showing a hole with several small hills at Kr ion irradiated graphite. Window of 286 × 286 nm^2. The linecut along the white line indicates the dimensions of the hole: depth of 0.6 nm, diameter of 20 nm.

Si samples were cut from 3″ commercial (100) wafer by cleaving. These samples of 1 × 1 cm^2 were irradiated perpendicular to the (100) plane. Irradiations were performed with 209 MeV Kr ions, available at the U-400 cyclotron of JINR, in Dubna. Special care was taken to avoid the sample surface contamination during sample preparation and irradiation, in order to perform measurements afterwards without any further sample manipulation (e.g. etching). Irradiations were carried out at room temperature, in a vacuum, with samples fixed onto a cooled metal surface. The ion flux was maintained at a relatively low level ($\approx 10^9$ ions/cm^2/s), thus temperature increase during the irradiation did not exceed 10–15°C. The ion fluence attained was 10^{12} ions/cm^2, in order to minimize cascade overlap in the surface region.

STM imaging was accomplished in constant current mode, in air, using tunnel current of 1 nA and a bias of 100 mV, with scanning speeds ranging from 100 to 3000 nm s^{-1}. Mechanically prepared Pt–Rh tips were used. Tapping mode AFM (Nanoscope III) was used for imaging surface features. Etched Si tips with resonance frequency in the range of 279 to 300 kHz were used. The curvature radius of the AFM tips were 70–80 nm.

In the case of all three materials one of the most characteristic type of features observed were hills with irregular shape and a wide distribution of size. Figs. 1 and 2 demonstrate this wide size dispersion, measured on graphite samples. In Fig. 1 atomic scale STM image proves that the size of the smallest hills is comparable to the atomic size. The regular corrugation in the lower left-hand corner of this figure corresponds to the graphite atomic order with 0.24 nm lattice parameter. Fig. 2 is a relatively large scale (1000 × 1000 nm^2) AFM image, demonstrating that the horizontal dimension of hills can extend up to hundreds of nanometers. These dimensions are considerable even if keeping in mind the distortion effect of the AFM tip, enlarging the horizontal measurements [13]. Using this figure, one can estimate the surface density of hills, although the smallest ones cannot be resolved in this image. Hence, the density must be somewhat higher than the approximately determined 5×10^9 features/cm^2 (5×10^{-3} features/ion) value.

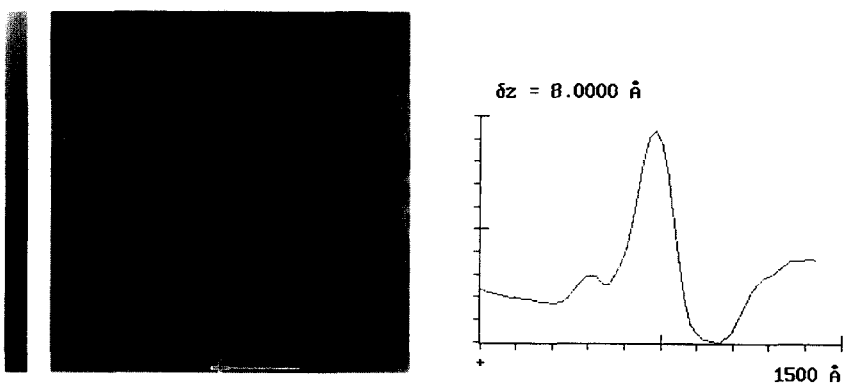

Fig. 6. STM image of two long tracks on Kr ion irradiated graphite. Window of 625 × 625 nm^2. The line cut, taken over the middle white line, shows the dimensions of the track: height of 0.8 nm, width of 30 nm.

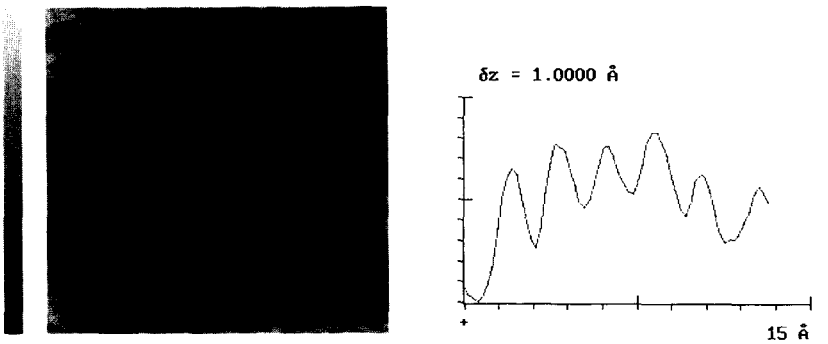

Fig. 7. Atomic resolution STM image on the top of the track shown in Fig. 6. Window of 5×5 nm^2. The line cut along the white line shows a graphite like atomic order.

Hills can be observed on Kr ion irradiated mica and silicon surface as well, as shown in Figs. 3 and 4, respectively. The horizontal dimensions of these hills range from 10 nm to some 100 nm. The heights of them extends up to 2 nm on silicon and to 20 nm on mica.

Furthermore, in some cases hills are closely grouped, as seen in Figs. 2 and 3, suggesting that they originate from the same event. In addition Fig. 2 also shows hills being frequently associated with one or more holes of different size. As pointed out before, variation of the apparent height in the AFM images, besides surface topography, can correspond to the stiffness variations, as well. Thus the nature of hole-like features cannot be determined merely by this AFM image. However, holes, with or without hills, can be observed by STM as well, which makes their topographic origin probable. Fig. 5 demonstrates such a hole imaged by STM on graphite sample with a diameter of 20 nm and a depth of 3.5 nm. The hole density, in the case of graphite was approximately 10^{10} holes/cm^2, determined by AFM images. The hole density was not measured in STM images.

Mica, being an insulating material, can be studied only by AFM. Holes have not been observed in these images in the case of perpendicular ion incidence, which does not exclude the existence of unresolved smaller ones. The situation is similar on the silicon samples in that sense that this material was studied only by AFM and holes have not been observed at normal ion incidence. However, it is to be noted that crater-like holes can be found if parallel Kr ion irradiation is carried out on Si samples. The morphology and the nature of the surface defects in this case are discussed in detail in a previous paper [14].

Besides hills and holes, the third characteristic type of features on graphite and mica surface, irradiated with Kr ions in perpendicular direction, is a long continuous track, parallel to the cleavage plane. The number of such tracks is much less than that of hills and holes; nevertheless, they can be found easily after irradiation at both of these layered materials. Typical examples of such tracks are seen in Fig. 6, observed by STM on graphite surface and in Fig. 8, detected by AFM on mica. As shown in Fig. 6, the length of the track is several hundreds of nanometers. The height of this feature is 0.8 nm over the intact surface. Its

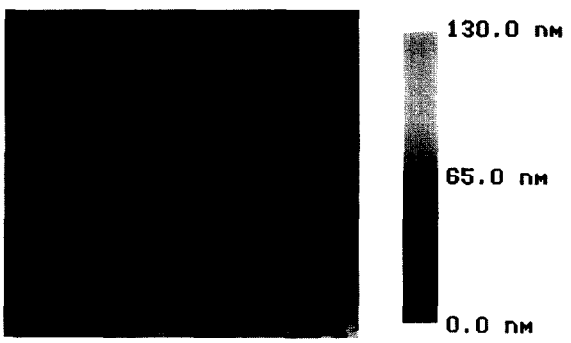

Fig. 8. AFM image of Kr ion irradiated mica showing branched track marked by an arrow. Window of 3×3 μm.

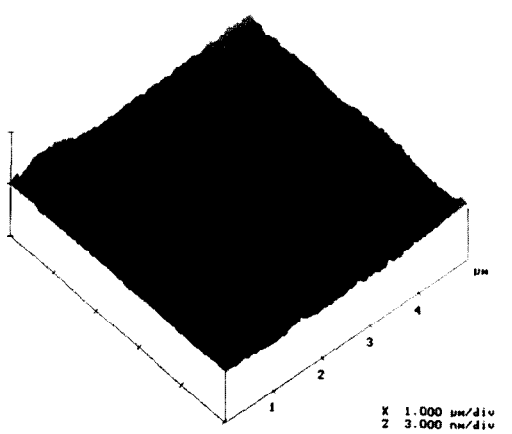

Fig. 9. Large scale AFM showing tracks parallel to the c plane of graphite irradiated with Kr ions. Horizontal scale of 1000 nm, vertical scale of 3 nm. Hills are seen on the left track. Both the tracks are branched.

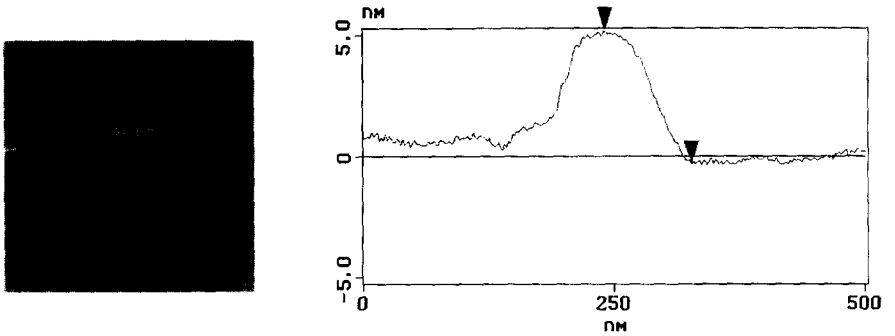

Fig. 10. AFM image of Kr ion irradiated graphite showing a track which ends in a hill. Window of 500 × 500 nm^2. The height of the hill is approximately 5 nm.

lateral extension is 30 nm, as shown by the line cut in Fig. 6. Very often the atomic order is not strongly disturbed on the top of tracks, which is demonstrated in Fig. 7 and by the line cut, taken over the track shown in Fig. 6. The corrugation along the line is near to the graphite atomic order, but it is bulging due to the track. At the same time one cannot superimpose one perfect graphite lattice over the whole image, showing that crumbled graphite like atomic order is found over the track surface. A several μm long track is shown in Fig. 8 imaged on mica surface. The track is marked by an arrow. Note the branching of the track above the arrow.

It is to be noted that such long tracks, lying parallel with the irradiated surface, could not have been observed on silicon surfaces.

A large scale AFM image helps a survey of the length of long tracks. Sometimes hills appear on them, as in Fig. 9. In other cases, the tracks branch off, as seen in Figs. 8 and 9 in the case of mica and graphite, respectively. In some cases the track terminates in a hill as in Fig. 10, taken by AFM on a graphite sample. In another case a track was observed to terminate in a hole, as has been shown earlier in a Ne ion irradiated graphite sample [11].

3. Discussion

The surface imaging of irradiated materials can provide an insight into the underlying physical processes. The first conclusion to be drawn from the perpendicular irradiation experiments above, is that there is no unambiguous evidence of entrance features of the impinging Kr ions. In the case of all three materials the overall density of visible surface features (for the most part hills and holes) is several orders of magnitude less than the impinging ion fluence, thus their production by electronic stopping effects, due to the impinging ions, can be ruled out. The electronic stopping power of 209 MeV Kr ions in Si, MM and graphite is in the range of 10 to 12 keV/nm. The threshold value of electronic stopping power for the visible entrance surface feature formation is probably greater than this value.

As far as the hills are concerned (Figs. 1–4), their irregular shape and wide size distribution, as well as the fact that often a central maximum is surrounded by small satellites, can be taken as an evidence supporting the idea of their nuclear collision origin. It is assumed that these type of features are the termination of nuclear cascades on the surface or somewhat below it. When some matrix atoms depart from the surface in the collision process a hole is connected to the hill. Analyzing the energy distribution of backsputtered matrix atoms in the case of swift heavy ions by means of TRIM code, it reveals that the most probable part ranges from some eV up to some hundreds of keV, which explains the large variation in size and shape of the measured surface features. The reason for failure observing holes on MM and Si surfaces in the case of perpendicular incidence is not yet clear. It is questionable whether this is because of the decreased resolution of our AFM imaging or because of some other physical explanation behind it.

We compared the measured density of surface features with computer calculations in the case of graphite. Simulations with TRIM code in the case of 209 MeV Kr ions yielded a value of backsputtered C atoms of 8.5×10^{-3} C atoms/ion. Taking into account the difficulty of density measurement, the simulated and measured densities seem to be in excellent agreement.

The existence of long tracks, parallel to the sample surface, i.e., the cleavage plane of the layered materials, raises two questions. What is the origin of this type of track and how can it be as long as it is observed? Since the irradiation direction was perpendicular to the sample surface, the projectile could hardly ever move parallel to the sample surface. This is practically excluded at such energies by the laws of the hard sphere collision model, which are applicable in this case. Consequently, these tracks must have been produced by knock-on target atoms of higher energy. Calculations, using the LET code [15], show that the primary knock-on atomic (PKA) spectrum of Kr ion

irradiated graphite and mica extends up to the MeV region. Thus, knock-on atoms with energies from 10 keV to 1 MeV, moving parallel to the cleavage plane, are realistic. A larger distance between the planes in these materials and the smaller electronic density make these planes a favourable channeling direction along which the energetic knock-on atoms are able to cover a much longer distance than in a random direction. The dissipated energy during the electronic stopping process, in this favoured direction, must be enough to separate the planes leading to the formation of the observed track. In other words, the threshold energy of the track formation must be anisotropic in these layered materials, being much less along the dense-packed layer than in the perpendicular direction. Nevertheless, the particular mechanisms of this separation process can be different in various layered materials.

Dechannelling can take place as the energetic particle passes along this favoured direction. As a consequence of dechannelling, nuclear collisions can take place along the path of the track. These collision processes explain that hills are found very often along the track as in Fig. 9, or branching is observed on it as seen in Figs. 8 and 9. Such a collision process can even terminate the travelling of the particle as shown in Fig. 10. Thus the same explanation can be cited in connection with hills or holes terminating the extension of a track.

4. Conclusions

The most characteristic surface features observed on HOPG, MM and Si after 209 MeV Kr ion irradiation are hills of irregular shape and wide size distribution. We attribute the origin of these features to the surface emergence of nuclear cascades.

The origin of the holes is less clear. Holes in perpendicular ion incidence were detected only on graphite, but not on mica and silicon surfaces. The explanation of the origin of the holes and the observed differences needs further efforts.

The long tracks observed merely at the layered irradiated materials are attributed to the anisotropic electronic stopping effect. The knocked-on target atoms can channel several microns along the densely packed layers while, as a consequence of the energy dissipation in the electronic cascade, the layers suffer deformation, resulting in the observed track. Hills, holes and branching along the tracks are attributed to dechannelling via nuclear collision.

There was no visible entrance feature of the bombarding Kr ions at neither of these materials indicating that the threshold energy of visible surface feature formation in random directions is higher than that in our case.

Acknowledgements

This work was supported by OTKA grant No. TO17344, Eötvös Hungarian State Fellowship and a special grant of the Hungarian Academy of Sciences to perform heavy ion irradiation at the Joint Institute for Nuclear Reactions, Dubna.

References

[1] A. Dunlop, D. Lesueur, A. Barbu, J. Nucl. Mater. 205 (1993) 426.
[2] R.L. Fleischer, P.B. Price, R.M. Walker, J. Appl. Phys. 36 (1965) 3645.
[3] D.A. Thomson, Radiat. Eff. 56 (1981) 105.
[4] G. Szenes, Phys. Rev. B51 (1995) 8026.
[5] R. Spohr, in: Ion Tracks and Microtechnology (Vieweg, Braunschweig, 1990) p. 224.
[6] L. Porte, M. Phaner, C.H. de Villeneuvre, N. Moncoffre, J. Tousset, Nucl. Instrum. Meth. B44 (1989) 116.
[7] S. Bouffard, J. Cousty, Y. Pennec, F. Thibaudau, Radiat. Eff. Def. Solids 126 (1993) 228.
[8] F. Thibaudau, J. Cousty, E. Balanzat, S. Bouffard, Phys. Rev. Lett. 67 (1991) 1582.
[9] L.P. Biró, J. Gyulai, K. Havancsák, Phys. Rev. B52 (1995) 2047.
[10] K. Havancsák, L.P. Biró, J. Gyulai, 18th Int. Conf. on Nuclear Tracks in Solids, 1–5 Sept. 1996, Cairo, Egypt, Radiat. Measurements, accepted.
[11] L.P. Biró, J. Gyulai, K. Havancsák, Nucl. Instrum. Meth. B112 (1995) 270–274.
[12] T. Hagen, S. Grafström, J. Ackerman, R. Neumann, C. Trautmann, J. Vetter, N. Angert, J. Vac. Sci. Technol. B12 (1994) 1555.
[13] L.P. Biró, J. Gyulai, K. Havancsák, A.Yu. Didyk, L. Frey, H. Ryssel, Nucl. Instrum. Meth. B112 (1997) 559.
[14] L.P. Biró, J. Gyulai, K. Havancsák, A. Yu. Didyk, S. Bogen, L. Frey, Phys. Rev. B (1996) 11853.
[15] G. Bárdos, Phys. Lett. A119 (1987) 415.